Cenozoic climate change as a possible cause for the rise of the Andes

Simon Lamb[1] **& Paul Davis**[2]

[1]*Department of Earth Sciences, Parks Road, Oxford, OX1 3PR, UK*
[2]*Department of Earth and Space Sciences, University of California, Los Angeles, California 90095, USA*

Causal links between the rise of a large mountain range and climate have often been considered to work in one direction, with significant uplift provoking climate change. Here we propose a mechanism by which Cenozoic climate change could have caused the rise of the Andes. Based on considerations of the force balance in the South American lithosphere, we suggest that the height of, and tectonics in, the Andes are strongly controlled both by shear stresses along the plate interface in the subduction zone and by buoyancy stress contrasts between the trench and highlands, and shear stresses in the subduction zone depend on the amount of subducted sediments. We propose that the dynamics of subduction and mountain-building in this region are controlled by the processes of erosion and sediment deposition, and ultimately climate. In central South America, climate-controlled sediment starvation would then cause high shear stress, focusing the plate boundary stresses that support the high Andes.

The Andes lie in the subducting plate boundary between the Nazca and South American plates, extending for more than 50° of latitude[1–3] (Fig. 1). They show remarkable systematic variations in both the maximum mean elevation and trench axial depth, with the greatest elevation contrasts between ~10° S and ~33° S (Fig. 2a), reaching ~13 km at ~24° S (ref. 1). In the high Andes, the high heat flow[4] and widespread late Cenozoic volcanism, together with very low Quaternary strain rates[5–8] ($<10^{-8}$ yr^{-1}), virtual absence of large earthquakes[6], and mixed strike-slip, oblique extension and fold and reverse fault Plio-Quaternary tectonics[6–13] (Fig. 2) strongly suggest that the lithosphere is weak and buoyancy stress contrasts, caused by elevation and density differences, must nearly be balanced by the available horizontal push in the South American lithosphere. In addition, if crustal shortening is the mechanism of uplift, then this push can never be less than the buoyancy stress in the highlands while they are rising, and it is transmitted across the subduction zone, where it is balanced by the shear stress along the plate interface[14].

Plate interface shear stress along the Andean margin

Figure 2 shows the mean lithospheric plate interface shear stress τ required to balance the buoyancy stress contrasts $\Delta\Gamma$ between the trench and high Andes, plotted as a function of latitude along the Peru–Chile trench. The calculated average shear stresses are in the range 10–50 MPa (for total buoyancy stress contrasts 30–140 MPa), in line with previous estimates of average shear stresses in subduction zones based on heat flow data[15–17]. At this stage, we do not distinguish between shear stresses in seismic or aseismic portions of the plate interface. The seismically active high-angle normal faults in the vicinity of the Cordillera Blanca at ~10° S (ref. 9)—where both focal mechanisms and the offset of Quaternary moraines point to extension more-or-less orthogonal to the range front[9,18], and possibly also extension farther south in the Puna[10]—suggest that the calculated shear stresses here may be too high (downward arrows in Fig. 2b). Conversely, reverse fault focal mechanisms in the high Andes at ~15° S, close to where the Nazca ridge is being subducted, suggest that the calculated shear stresses here are too low (upward arrow in Fig. 2b).

If the actual shear stresses everywhere were in fact more-or-less the same, then the high Andes would have to be supporting horizontal deviatoric stresses between 30 and 55 MPa averaged over the entire thickness of the lithosphere, either extensional in the Central Andes, or compressional elsewhere. From the previous discussion, we do not consider this plausible (Fig. 2a). Also, a pronounced flexural outer bulge between ~15° and 25° S in the Nazca plate[19], adjacent to the trench, suggests that the oceanic lithosphere is bending under higher horizontal compression here than elsewhere along the Andean margin. More evidence comes from a consideration of the thermal structure of the subduction zone.

Thermal modelling shows that the temperature at any depth on the plate interface, T, is proportional to the sum of the heat flux (q_0) from the subducted oceanic plate and shear heating τV (frictional or viscous dissipation) along the plate interface, for subduction at velocity V (refs 15, 16). In this case, given our calculated shear stresses τ (Fig. 2b) and relevant subduction parameters[3,20–23] (Fig. 2) between 0 and 45° S (Fig. 1), we predict that the thermal structure does not change significantly with latitude, with a nearly constant combined average heat-source term ($q_0 + \tau V$) of ~160 mW m^{-2} (Fig. 3) because enhanced shear heating in the high shear stress segments more-or-less compensates for the lower heat flux from older oceanic lithosphere—the blanketing effect of trench sediment may also help to keep this balance (see below). If the down-dip edge of the seismogenic zone is defined by an isotherm[24], then the remarkably constant depth of ~50 km to this edge along the Andean margin for the 1995 magnitude $M = 8$ Antofagasta earthquake between 22° and 26° S (ref. 21), as well as pre-1995 seismicity here[6], and the 1960 $M = 9+$ Concepçion earthquake between 36° S and ~45° S (ref. 22), with no clear overall trend elsewhere[17], strongly supports this prediction. The predicted downward heat advection[15] is also consistent with the observed mean forearc heat flow[4] (~30 mW m^{-2}) in northern Chile.

We conclude that all these observations require a focusing of the plate-boundary push along the Andean margin between 10° S and 33° S, because here the buoyancy stress or potential energy per unit volume contrast between the trench and high Andes is higher than elsewhere (Fig. 2b, >100 MPa). This does not depend on other effects, such as enhanced or retarded erosion[25], or rheology of the South American lithosphere, because we are considering a vertical and horizontal stress balance in the high Andes where both strain rates and deviatoric stresses are very small, so that rheological effects are negligible.

Trench sediment fill and subduction dynamics

The systematic variations in plate interface shear stresses needed to support the maximum elevation and buoyancy stress contrasts in

the Andes must be a consequence of latitudinal variations in the coefficient of friction or pore fluid pressure on the seismogenic plate interface (normal stress variations are negligible) and/or viscosity or yield strength in the viscous/plastic zone. In view of the discussion above, we believe that the only plausible explanation is some compositional or lithological change in the nature of the plate interface that varies on a length scale of ~1,000 km—other factors such as the presence of aseismic ridges, the relative plate convergence velocity or direction, or the age of the subducted plate, either do not vary at all significantly, or do not vary in the necessary way or on the appropriate length scale. We believe that the presence or absence of significant trench sediment fill provides the best explanation for lithological or compositional variations in the plate interface on the appropriate length scale.

Along the Andean margin between 10° S and 33.5° S, it is striking that the trench is virtually starved of sediment, with either none or <500 m, where calculated plate interface shear stresses >35 MPa, but this fill is generally 1–2.5 km thick where shear stresses are much less[26,27] (Fig. 2b). It is particularly interesting, in this respect, that the zone of seismically active normal faulting in the high Andes at ~10° S, where there is a significant decrease in shear stresses, coincides with a marked increase in the thickness of the trench sediment fill[26] (Fig. 2b). We recognize, however, that this is merely a snapshot in time, and the trench could be tectonically cleaned out in <1 Myr (ref. 28). We argue (see below) that though trench sediment fill may be episodic, the present sediment distribution is representative of the average fill extending at least into the Pliocene and probably much older[28]. For example, a longer-term history of subduction erosion in the sediment starved segments, manifested in the extreme trenchward position of early Cenozoic era to Jurassic period volcanic arcs between ~16° and 26° S (ref. 29; Fig. 2a), could be attributed to earlier periods of sediment starvation, though it is unclear from the position of the Neogene volcanic arc in the Central Andes whether there has been any net trench migration in the last ~25 Myr (ref. 29).

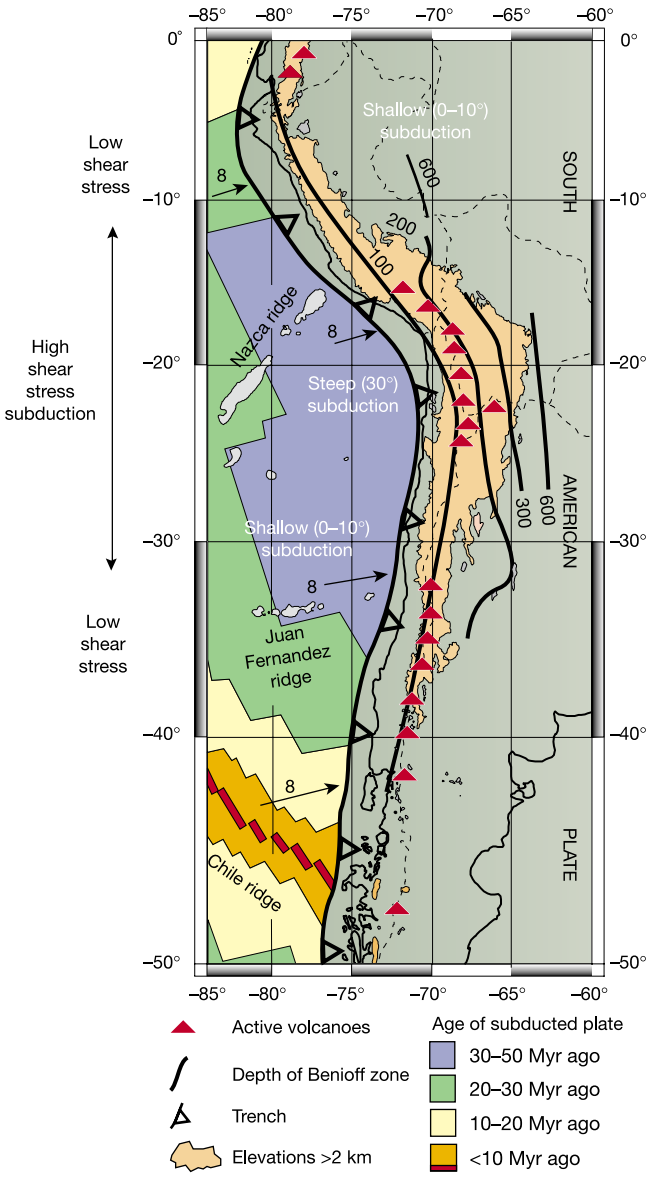

Figure 1 Tectonic map of the Andean plate margin along the western side of South America between 0 and 50° S. Shown are the age and geometry of the subducting Nazca plate[2,3] and the location of the volcanic arc and regions with elevations >2,000 m in the South American plate[1]. Depth of Benioff zone is given in km.

In the sediment-starved sections, where there is no extensive or thick blanketing of the rough oceanic basaltic basement, and tectonic erosion may have been active, significant portions of the plate interface could be between relatively strong basalt in the oceanic plate and relatively dry mafic and felsic basement rocks in the overlying prism[16], with relatively low pore fluid pressures and minimal lubrication from fine-grained subducted trench sediments[16,30]. All this would promote higher shear stresses compared to segments of the trench where layered turbidite sequences, up to 2.5 km thick, smooth out the top of the subducting plate and provide an abundant source of weak water-rich lubricating material along the plate interface. However, this simple picture has been complicated by the discovery that the sediment-starved margin in northern Chile may be ingesting water-rich sediments[31]. This is because the subduction of rough oceanic topography can erode and undermine the toe of the overriding plate, steepening the slope of the prism and triggering extensive slumps and debris flows which are dragged along the plate interface.

We suggest that the chaotic debris cannibalized from the plate toe does not have the same lubricating effect as the well-stratified and finer-grained trench sediment fill that has smoothed out oceanic basement topography before being subducted. The cannibalized sediment may also be accumulating near the tip of the seismogenic zone, before eventually rising up through the prism as extensive slumping strips off the surface (Fig. 3a)—this may be responsible for limiting the up-dip extension of the seismogenic zone, which is here several kilometres deeper than along the southern Chilean margin[31]. Such a process, as well as reducing, or even preventing, the ingestion of water and trench sediment into deeper parts of the subduction zone (where tectonic erosion of the plate interface may be eating into the basement of the overlying prism), will help cool the up-dip parts of the plate interface by advecting heat upwards, further counteracting the warming and weakening effects of shear heating. Conversely, in sediment-rich trenches, the blanketing of the trench in several kilometres of sediment will raise oceanic basement temperatures near the toe of the overriding prism by up to 100 °C (ref. 24, for Andean subduction parameters), which would make up for any thermal deficit from reduced shear heating, without important surface slumping so that sediment is carried much farther down the plate interface (Fig. 3b).

An association between excess trench sediments and great earthquakes[32] provides further evidence for the role of trench sediments in subduction dynamics. The two largest subduction earthquakes ever recorded instrumentally—the $M = 9+$ 1960 Concepçion and 1964 Alaskan earthquakes—ruptured sediment-rich parts of the trench, with similarly low (10–20 MPa) average plate interface shear stresses[33]. The simplest explanation is that the sediment smoothes out the stress distribution and lubricates the plate interface, allowing the earthquake to propagate over a wide area of the fault plane

once the major asperity barrier is broken[32]. For sediment-starved trenches the stress distribution is much rougher and earthquakes tend to be smaller[32]. Clearly, the largest earthquakes do not require the highest average shear stresses—it is the stress coherency that is important. Furthermore the mean stress drop associated with the 1960 Concepçion event (1–2 MPa) was small, ~10% of our calculated ambient shear stress[22].

The present sediment-starved nature of the Peru–Chile trench is a direct consequence of the arid climate along the west coast of this portion of South America[26,34,35] (Figs 2a, 4). There is virtually no run-off into the Pacific at these latitudes—the pelagic sedimentary component is likely to be negligible (tens to hundreds of metres) for this age of oceanic lithosphere and at depths below the carbonate compensation depth. That the arid coastal climate plays such an overriding control is also due to the fact that the Andes form an unbroken watershed for most of their length, so that no drainage from the wetter eastern parts of South America reaches the Pacific coast. However, where the coastal climate is significantly wetter, south of ~31° S, there is some northward transport of sediment along the trench axis by axial turbidite flows, with thicknesses up to 500 m reaching as far north as ~28° S, although the Juan Fernandez ridge may also have acted as a local sediment barrier[26,27] (Fig. 2a). Likewise, axial sediment flow at low latitudes has transported sediment along the trench as far south as ~12° S (ref. 26) (Fig. 2a).

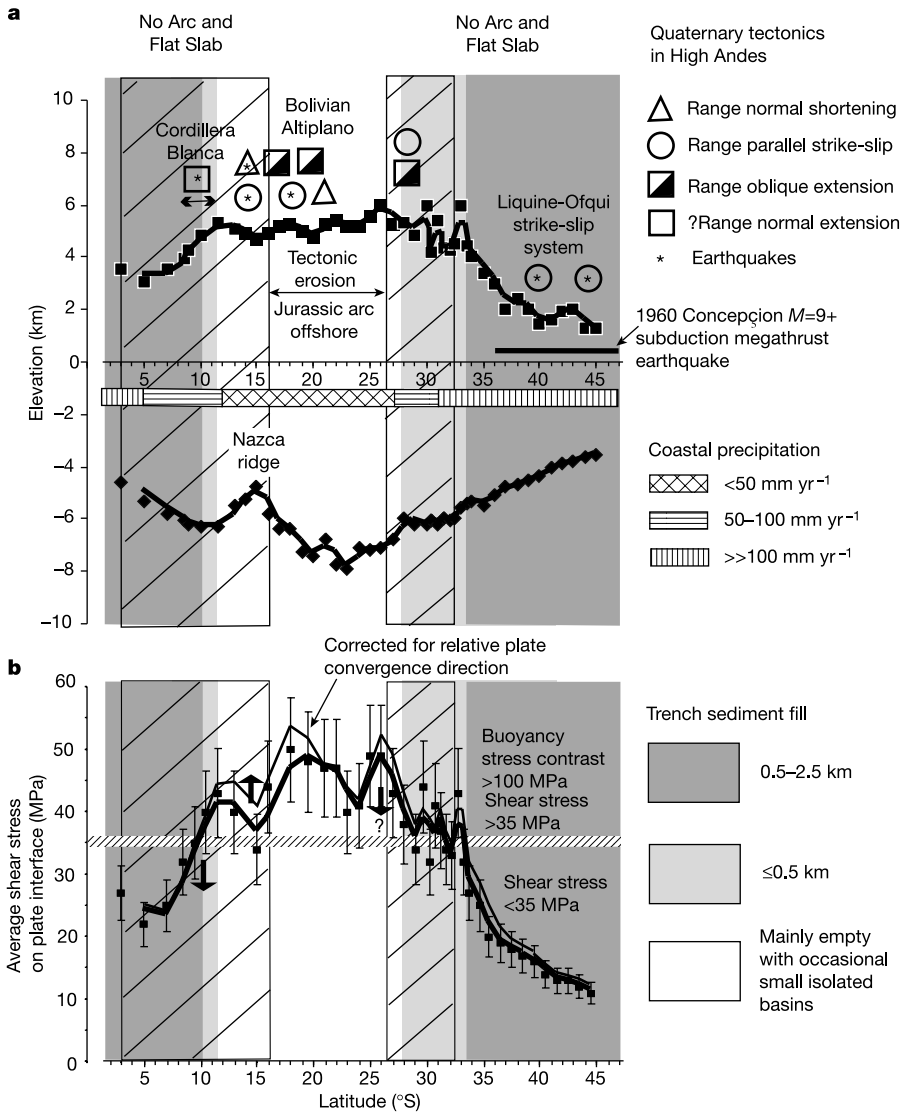

Figure 2 Plots showing latitudinal variations along the length of the Peru–Chile trench between ~3° to 46° S (ref. 1). Information from the Andes has been projected along directions normal to the trench. **a**, Average maximum elevations of high Andes and maximum depth of trench (averaged over 30 km length scale normal to trench, plotted here with a two-point running average curve fit), with the main features of Quaternary tectonics in high Andes, and coastal precipitation. Note the rupture zone of the $M = 9+$ 1960 Concepçion earthquake between 36° and 46° S[22], evidence for tectonic erosion between 16° and 26° S[29], and location of flat slab segments in the subduction zone[3]. **b**, Shear stresses (τ) on the plate interface[14] required to balance buoyancy stress contrasts ($\Delta\Gamma$) between the trench and high Andes, calculated from a simple one-dimensional analysis across the subduction zone using the method of ref. 51 with appropriate crustal[52] and lithospheric parameters ($\rho_{crust} = 2.85\,g\,cm^{-3}$, $\rho_{mantle} = 3.25\,g\,cm^{-3}$, maximum depth of interplate coupling[20] = 85 ± 5 km, reference crustal thickness = 37.5 ± 5, Moho intersection of subduction zone = 45 ± 5 km, plate interface dip[3,20–22] = 20 ± 5°). This approach is permissible because the width-to-length aspect ratio of the Andean ranges is $\ll 1$ so that along-length gradients of shear stress are small. A small correction for the deviation of subduction from orthogonal[23] (<30°) gives an upper acceptable estimate of shear stress. The curve fit is a two-point (100 km scale) running average. Error bars show approximate 1-sigma uncertainties (~17%), each based on 1,000 random trials. Portions of the trench where $\Delta\Gamma > 100$ MPa, $\tau > 35$ MPa coincide with either no or very thin (<500 m) axial sediment fill[26,27].

Climate change and Andean tectonic evolution

If we are right that the buoyancy stress contrasts in the Andes can only be supported because of the role of climatically controlled trench sediment fill, then it is important to ask whether these elevation contrasts could have existed in the past when the global climate was significantly different. Both the Nazca–South America relative plate convergence history and the inherited rheology of the South American lithosphere have often been invoked as primary controls of the Cenozoic tectonic evolution of the Andes[5,10,13,14,36–38], although phases of intense behind-arc shortening seem to correlate better with periods of slow rather than fast convergence[23,36,37,39] (Fig. 5f)—possibly because slower convergence will result in a cooler plate interface by reducing any shear heating[16].

Inherited rheological effects can certainly influence the rate, amount and distribution of deformation if deviatoric stresses are significant[5,14], but unless they lead to a change in the plate interface shear stress or trench-highland buoyancy stress contrast, as previously described, they cannot determine the maximum elevations of the high Andes or the timing of deformation. A wider zone of weaker lithosphere may be part of the explanation for the width and amount of deformation in the Central Andes[10,14] but it does not explain the higher mountains here, which require higher horizontal normal stresses and more lateral support at the plate interface. Indeed, there is no systematic overall correlation between the elevations, amount of deformation and width of the Andes—high elevations are found as far south as 33° S, and as far north as 12° S, where the widths are only a fraction of those around 20° S (compare Figs 1 and 2a). For this reason, given our previous conclusions, we believe that the global cooling of the climate and deep ocean[40] (Fig. 5a) must be considered as another important effect on the tectonic evolution.

The extreme arid climate of northern Chile and Peru (precipitation $<50\,\mathrm{mm\,yr^{-1}}$, see Figs 2a, 4), is a consequence of both atmospheric and ocean circulation, as well as the more local rain shadow effect of the Central Andes themselves, blocking flow of moist air from farther east, in the Amazon region[35,41]. The cold Peru–Chile current system[42] (PCC) and wind-driven coastal upwellings[35] play an important role in maintaining this aridity by significantly lowering the near-shore air temperature (Fig. 4) and effectively starving any sea-derived winds of moisture, as well as suppressing the rising of and precipitation from the air column[35].

An eastern boundary current system, with associated upwellings, has flowed along the western margin of South America since at least the earliest Cenozoic[43]. However, the temperature of both shallow- and deep-water masses must have been strongly influenced by cooling around Antarctica. This led to enhanced oceanographic and latitudinal temperature gradients[44] and a northward shift and strengthening of the Antarctic circumpolar current (ACC), resulting in stronger northward advection of cold subpolar water into the southern PCC. In this case, the large expansion of the East (at ~14 Myr) and West (at ~6 Myr) Antarctic ice sheets, after the mid-Miocene climatic optimum[40], signal a pronounced cooling of both

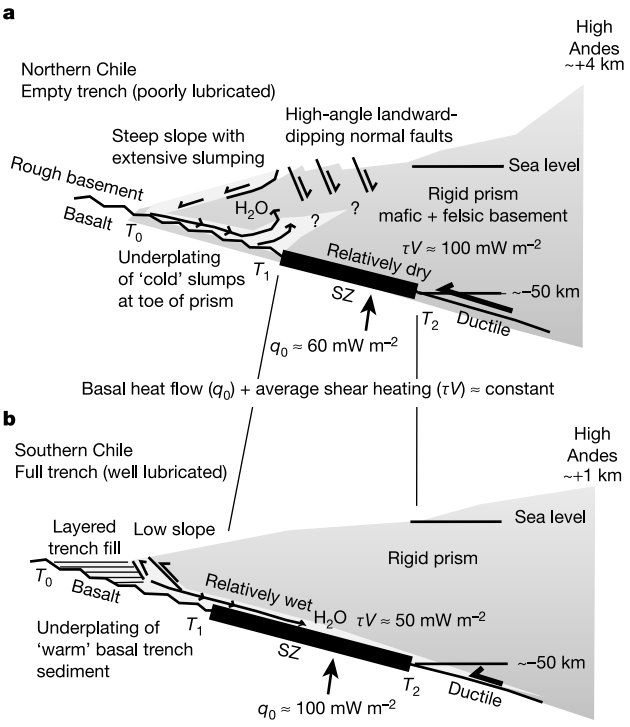

Figure 3 Two cartoons illustrating how the presence or absence of significant trench fill could affect the process of subduction. In both cases, the convergence velocity V, and the combined heat derived both from the subducted plate (q_0) and average shear heating along the plate interface (τV) is more-or-less the same. The seismogenic zone (SZ) is assumed to be defined by isotherms T_1 and T_2, with T_2 generally lying at ~50 km. **a**, Extensive undermining of the toe of sediment-starved trenches, such as that in northern Chile, may drag chaotic and coarse debris into the subduction zone, but this probably accumulates and rises near the up-dip edge of the SZ as slumping strips off the overlying prism, helping to cool the plate interface as well as limiting further down-dip movement of the sediment. High-angle landward-dipping normal faults, typical of this type of margin, may be the coastal expression of this. **b**, Trenches full of well-stratified fine-grained sediment may result in 'well-lubricated' and smooth[32] subduction zones because the wet sediment may form a weak detachment extending far down the plate interface. Blanketing of the oceanic basement by sediment will also help to warm the subducted oceanic basement.

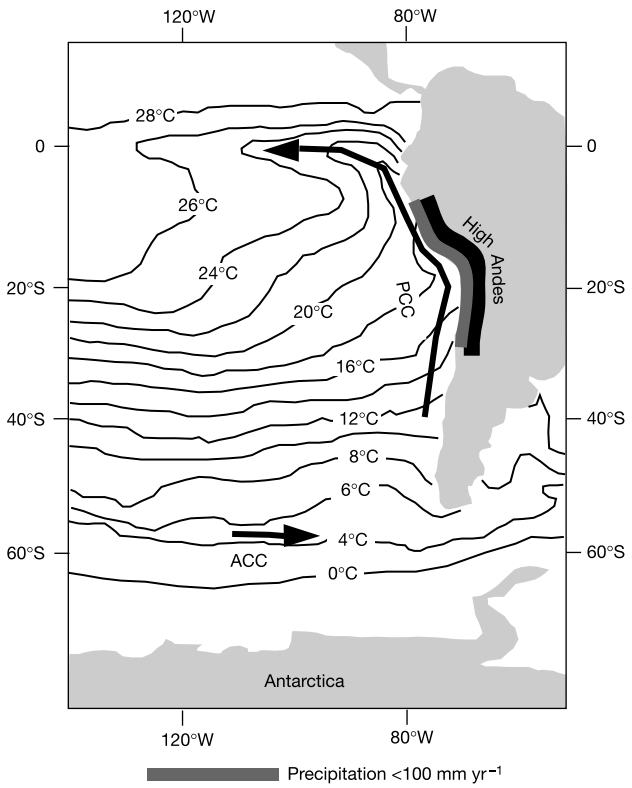

Figure 4 The Peru–Chile current system[42] and the associated wind-induced oceanic upwelling can be clearly seen in the sea surface temperatures (interpolated satellite and *in situ* measurements from NOAA website: www.nodc.noaa.gov) for July 2002—a tongue of water nearly 8 °C colder than that at equivalent latitudes farther west extends up the west coast of South America. This plays an important role in limiting precipitation at mid-latitudes along the coast, where the Andes are highest and widest. The Antarctic circumpolar current flows round Antarctica.

the PCC and deep Pacific water, when the global climate was also cooling (Fig. 5a–c). This seems to correlate remarkably well with the available evidence for the most rapid phase of surface uplift and shortening ($\sim$10 mm yr^{-1}) in the behind-arc region of the central Andes[5,13,45] (Fig. 5d, e). Intense shortening in the sub-Andean zone initiated in the mid- to late-Miocene (10–20 Myr) with >100 km of underthrusting of the Brazilian shield[13,38,46] (Fig. 5e), and 1–3 km of surface uplift in the Bolivian Altiplano and Eastern Cordillera, so that by the Plio-Pleistocene epoch average elevations exceeded 3 km for the first time[13,46,47].

We suggest that the cooling of the PCC (possibly in combination with essentially synchronous planetary cooling[40,41,44]) provides the causal link between climate change and Andean tectonics, triggering the Mio-Pleistocene trend towards increased aridity along the west coast of South America, which resulted in hyperaridity in the last 3–4 Myr (ref. 41). This aridity was necessary to greatly reduce or cut off the sediment supply to the trench, depriving the plate interface of its lubrication and raising shear stresses to the levels required to push up and support the high Andes. Judging from Fig. 2, these effects seem to become important once the trench fill drops below $\sim$500 m—this may reflect the sediment required to smooth oceanic basement topography. Strong positive feedbacks between uplift, strengthening of the southeastern Pacific anticyclone, and the development of a pronounced orographic barrier to moist air from the Amazon basin, would have further promoted the increasing aridity, making this region even more sensitive to the forcing of global climate change.

We speculate that a rise in plate-interface shear stresses could also have occurred in the Eocene, associated with the onset of Cenozoic cooling[40] (Fig. 5a). The pre-Miocene climate along the west coast of South America is largely unknown. However, the Eocene to Miocene eastward migration of the volcanic arc[29] can be explained by sediment starvation and tectonic erosion in the trench. Thus, it is plausible that the late Eocene initiation of intense back-arc shortening in the Bolivian Andes, around $\sim$40 Myr, when the main behind-arc ranges of the central Andes first started to rise[13,48,49] (Fig. 5e, f), may be a consequence of enhanced shear stresses along the plate interface, caused at least in part by coastal aridity and trench sediment starvation in the Eocene as a consequence of global cooling[40]. Another possible factor is flattening of the slab between $\sim$35 and 25 Myr (Fig. 5e), associated with the shutting off of the volcanic arc at this period[13,48], but the lack of any systematic relation between the present flat slab regions and Andean topography (Fig. 2a) suggests that this is probably not very significant.

We conclude that high mountain ranges like the central Andes

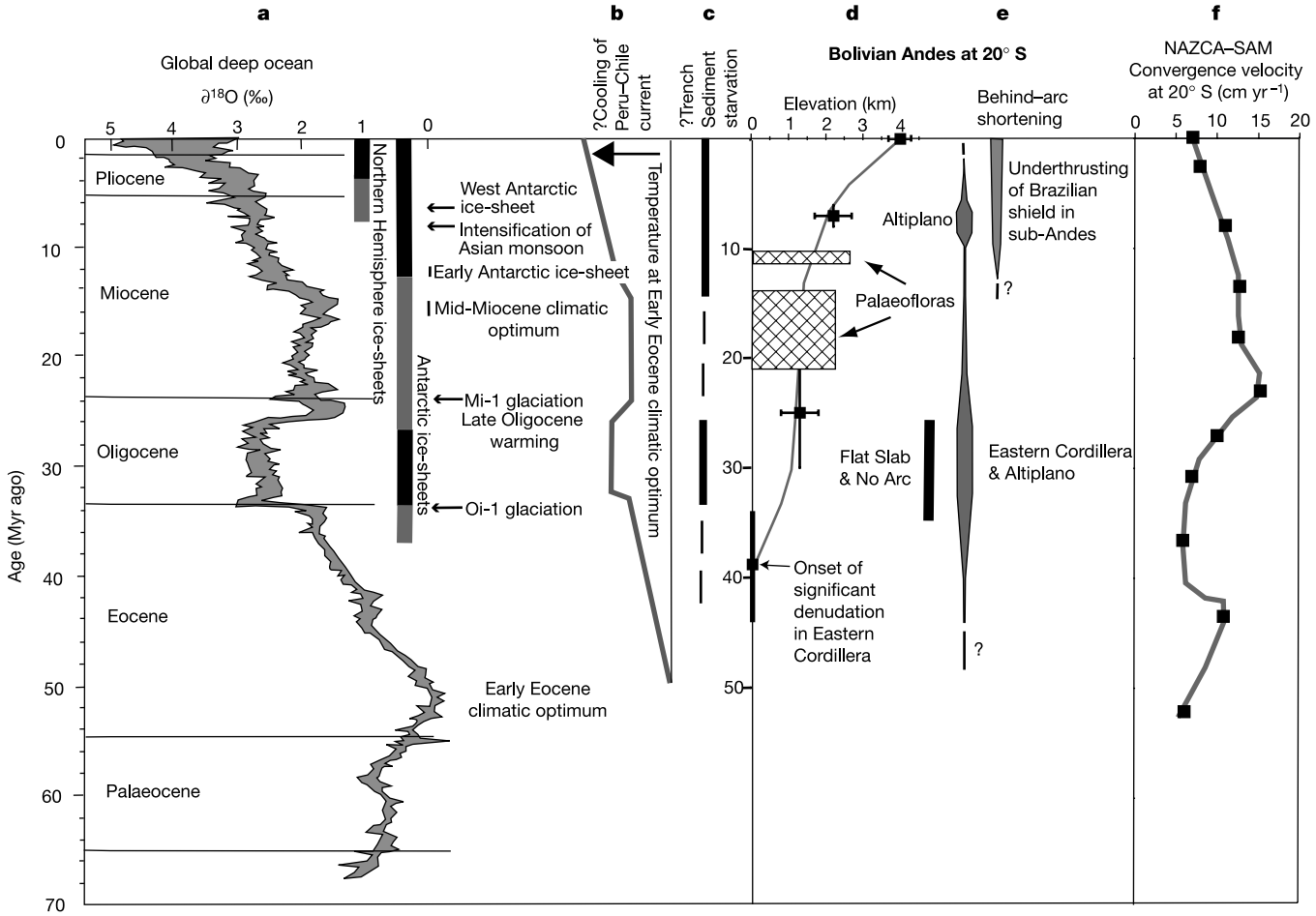

Figure 5 Major global climatic trends, and Andean tectonic evolution at $\sim$20° S, compiled from various sources. **a**, Long-term trends in benthic oxygen isotope ratios[40], reflecting both cooling of the deep ocean and changes in ice volumes. **b**, Postulated trend in the general surface water temperatures in the Peru–Chile current system. **c**, Postulated phases of sediment starvation in the Peru–Chile trench along the central Andes during periods of high coastal aridity. **d**, **e**, Mean elevation history of the Altiplano and western margin of the Eastern Cordillera in the Bolivian Andes, based on a self-consistent inversion of estimates from geomorphological data[13,45] combined with crustal-thickening estimates and their timings[47–49] from crustal-shortening data[13,52], which are broadly in line with palaeobotanical constraints[47] (shown by cross-ruled boxes), though there are still significant uncertainties. **f**, The absolute relative convergence velocity[36,37] at 20° S between the South American (SAM) and Nazca plates (NAZCA)—note the slow-down in the last $\sim$25 Myr, and also between 40 and 45 Myr.

may not be typical features of active plate margins, but restricted to regions where climatic conditions are right. The climate here, by promoting or inhibiting sedimentation, may help to focus the available plate-driving forces to relatively restricted portions of subducting plate boundaries, raising the local shear stresses to levels needed to support mountain belts with elevations >3 km. For example, if the Atlantic mid-ocean-ridge push is the main driving force in the Andes, then without some sort of focusing, it would not be expected to support mountains higher than 0.5 to 2.0 km (ref. 50). Finally, an increase in plate interface shear stresses might be a significant driving force for phases of relative plate motion deceleration. □

Received 21 March; accepted 12 September 2003; doi:10.1038/nature02049.

1. Digital Elevation Model (3m × 3m) of South America (Getech, Univ. Leeds, Leeds, UK, 1998).
2. Muller, R. D., Roest, W. R., Royer, J.-Y., Gahagan, L. M. & Sclater, J. G. Digital isochrons of the world's ocean floor. *J. Geophys. Res.* **102,** 3211–3214 (1997).
3. Cahill, T. & Isacks, B. L. Seismicity and shape of the subducted Nazca plate. *J. Geophys. Res.* **97,** 17503–17529 (1992).
4. Springer, M. Heat-flow density across the Central Andean subduction zone. *Tectonophysics* **291,** 123–139 (1998).
5. Lamb, S. H. Active deformation in the Bolivian Andes, South America. *J. Geophys. Res.* **105,** 25627–25653 (2000).
6. National Earthquake Information Center (NEIC) *Earthquake Catalogue* (World Data Centre for Seismology, United States Geological Survey, Denver, 2003).
7. Mercier, J. L. *et al.* Changes in the tectonic regime above a subduction zone of Andean type: the Andes of Peru and Bolivia during the Plio-Pleistocene. *J. Geophys. Res.* **97,** 11945–11982 (1992).
8. Suarez, G., Molnar, P. & Burchfiel, B. C. Seismicity, fault plane solutions, depth of faulting, and active tectonics of the Andes of Peru, Ecuador, and Southern Columbia. *J. Geophys. Res.* **88,** 10403–10428 (1983).
9. Schwartz, D. Paleoseismicity and neotectonics of the Cordillera Blanca Fault Zone, Northern Peruvian Andes. *J. Geophys. Res.* **93,** 4712–4730 (1988).
10. Allmendinger, R. W., Jordan, T. E., Kay, S. M. & Isacks, B. L. The evolution of the Altiplano Plateau of the Central Andes. *Annu. Rev. Earth Planet. Sci.* **25,** 139–174 (1997).
11. Cembrano, J., Herve, F. & Lavenu, A. The Liquine Ofqui fault zone: a long lived intra-arc fault system in southern Chile. *Tectonophysics* **259,** 55–66 (1996).
12. Cladouhos, T., Allmendinger, R., Coira, B. & Ferrar, E. Late Cenozoic deformation in the central Andes: Fault kinematics from the northern Puna, northwestern Argentina and southwestern Bolivia. *J. Soc. Am. Earth Sci.* **7,** 209–228 (1994).
13. Lamb, S. H. & Hoke, L. Origin of the high plateau in the central Andes, Bolivia, South America. *Tectonics* **16,** 623–649 (1997).
14. Lamb, S. H. Vertical axis rotation in the Bolivian orocline, South America, 2: Kinematic and dynamical implications. *J. Geophys. Res.* **106,** 26605–26632 (2001b).
15. Molnar, P. & England, P. Temperatures, heat flux, and frictional stress near major thrust faults. *J. Geophys. Res.* **95,** 4833–4856 (1990).
16. Peacock, S. in *Subduction, Top to Bottom* (eds Bebout, G. E. *et al.*) 119–133 (Geophys. Monogr. 96, American Geophysical Union, Washington, 1996).
17. Tichelaar, B. W. & Ruff, L. J. Depth of seismic coupling along subduction zones. *J. Geophys. Res.* **98,** 2017–2037 (1993).
18. Doser, D. I. The Ancash, Peru, earthquake of 1946 November 10: evidence for low-angle normal faulting in the high Andes of northern Peru. *Geophys. J. R. Astron. Soc.* **91,** 57–71 (1987).
19. Judge, A. V. & McNutt, M. Curvature and elastic plate thickness in the Peru-Chile trench. *J. Geophys. Res.* **96,** 16,625–16,640 (1991).
20. Delouis, B. *et al.* The Andean subduction zone between 22 and 25°S (northern Chile): precise geometry and state of stress. *Tectonophysics* **259,** 67–80 (1996).
21. Klotz, J. *et al.* GPS-derived deformation of the Central Andes including the 1995 Antofagasta Mw = 8.0 Earthquake. *Pure Appl. Geophys.* **154,** 709–730 (1999).
22. Barrientos, S. E. & Ward, S. N. The 1960 Chile earthquake: inversion for slip distribution from surface deformation. *Geophys. J. Int.* **103,** 589–598 (1990).
23. Angermann, D., Klotz, J. & Reigber, C. Space-geodetic estimation of the Nazca-South America Euler vector. *Earth Planet. Sci. Lett.* **171,** 329–334 (1999).
24. Hyndman, R. D. & Wang, K. Thermal constraints on the zone of major thrust earthquake failure: The Cascadia Subduction Zone. *J. Geophys. Res.* **98,** 2039–2060 (1993).
25. Montgomery, D. R., Balco, G. & Willet, S. D. Climate, tectonics, and the morphology of the Andes. *Geology* **29,** 579–582 (2001).
26. Kulm, L. D., Schweller, W. J. & Masias, A. in *Island Arcs, Deep Sea Trenches and Back-Arc Basins* (eds Talwani, M. & Pitman, W. C. III) 285–301 (Maurice Ewing Ser. 1, American Geophysical Union, 1977).
27. Thornburg, T. & Kulm, L. D. Sedimentation in the Chile Trench: Depositional morphologies, lithofacies, and stratigraphy. *Bull. Geol. Soc. Am.* **98,** 33–52 (1987).
28. Bangs, N. L. & Cande, S. C. Episodic development of a convergent margin inferred from structures and processes along the southern Chile margin. *Tectonics* **16,** 489–503 (1997).
29. Giese, P., Reutter, K. J. & Scheuber, E. *Welche Prozesse haben die Entstehung der extremen Dimensionen der zentralen Anden verursacht? Deformationsprozesse in den Anden* 15–34 (Sonderforschungsbereich 267, Freie Univ. Berlin/Tech. Univ. Berlin/GeoForschungsZentrum Potsdam/Univ. Potsdam, Berlin, 1998).
30. von Huene, R. & Scholl, D. W. Observations at convergent margins concerning sediment subduction, subduction erosion, and the growth of continental crust. *Rev. Geophys.* **29,** 279–316 (1991).
31. von Huene, R. & Ranero, C. R. Subduction erosion and basal friction along the sediment-starved convergent margin of Antofagasta, Chile. *J. Geophys. Res.* **108,** 2079, doi:10.1029/2001JB001569 (2003).
32. Ruff, L. J. Do trench sediments affect great earthquake occurrence in subduction zones? *Pure Appl. Geophys.* **129,** 263–282 (1989).
33. Gutscher, M. A. & Peacock, S. M. Thermal models of flat subduction and the rupture zone of great subduction earthquakes. *J. Geophys. Res.* **108**(B1), 2009, doi:10.1029/2001JB000787 (2003).
34. Clapperton, C. *Quaternary Geology and Geomorphology of South America* (Elsevier, Amsterdam, 1993).
35. Schwertfelder, W. (ed.) *Climates of Central and South America* 1–532 (Elsevier, New York, 1976).
36. Pardo-Casas, F. & Molnar, P. Relative motion of the Nazca (Farallon) and South American plates since Late Cretaceous time. *Tectonics* **6,** 233–248 (1987).
37. Somoza, R. Updated Nazca (Farallon)–South America relative motions during the last 40 My: implications for mountain building in the central Andean region. *J. Soc. Am. Earth Sci.* **11,** 211–215 (1998).
38. Watts, A., Lamb, S., Fairhead, J. & Dewey, J. F. Lithospheric flexure and bending of the central Andes. *Earth Planet. Sci. Lett.* **134,** 9–21 (1995).
39. Hindle, D. *et al.* Consistent geologic and geodetic displacements during Andean orogenesis. *Geophys. Res. Lett.* **29,** 3757–3761 (2002).
40. Zachos, J., Pagani, N., Sloan, L., Thomas, E. & Billups, K. Trends, rhythms, and aberrations in the global climate 65 Ma to present. *Science* **292,** 686–693 (2001).
41. Hartley, A. J. Andean uplift and climate change. *J. Geol. Soc. Lond.* **160,** 7–10 (2003).
42. Strub, P. T. *The Sea–Global Coastal Ocean, Regional Studies and Syntheses.* (eds Robinson, A. R. & Brink, K. H.) 273–315 (Wiley, New York, 1998).
43. Keller, G. *et al.* The Cretaceous/Tertiary boundary event in Ecuador: reduced biotic effects due to the eastern boundary current setting. *Mar. Micropaleontol.* **31,** 97–133 (1997).
44. Rind, D. Latitudinal temperature gradients and climate change. *J. Geophys. Res.* **103**(D6), 5943–5971 (1998).
45. Gubbels, T. L., Isacks, B. L. & Farrar, E. High-level surfaces, plateau uplift, and foreland basin development, Bolivian central Andes. *Geology* **21,** 695–698 (1993).
46. Lamb, S. H. Vertical axis rotation in the Bolivian orocline, South America, 1: Paleomagnetic analysis of Cretaceous and Cenozoic rocks. *J. Geophys. Res.* **106,** 26633–26653 (2001a).
47. Gregory-Wodzicki, K. M. Uplift history of the Central and Northern Andes: A review. *Bull. Geol. Soc. Am.* **112,** 1091–1105 (2000).
48. Lamb, S. H., Hoke, L., Kennan, L. & Dewey, J. in *Orogeny Through Time* (eds Burg, J.-P. & Ford, M.) 237–264 (Geol. Soc. Spec. Publ., Geological Society of London, UK, 1997).
49. Horton, B. K., Hampton, B. A., LaReau, B. N. & Baldellon, E. Tertiary provenance history of the northern and central Altiplano (central Andes, Bolivia): A detrital record of plateau margin tectonics. *J. Sedim. Res.* **72,** 711–726 (2002).
50. Crouch, S. T. Rifts and swells: Geophysical constraints on causality. *Tectonophysics* **94,** 23–37 (1983).
51. Smith, A. G. in *Thrust and Nappe Tectonics* (eds McClay, K. R. & Price, N. J.) 111–124 (Geol. Soc. Spec. Publ. 9, Geological Society of London, UK, 1981).
52. Beck, S. *et al.* Crustal thickness variations in the central Andes. *Geology* **24,** 407–410 (1996).

Acknowledgements This work was supported by grants from the European Union, Natural Environment Research Council, and Royal Society (S.H.L.) and a visiting Leverhulme professorship (P.D.).

Competing interests statement The authors declare that they have no competing financial interests.

Correspondence and requests for materials should be addressed to S.H.L. (simon.lamb@earth.ox.ac.uk).